Ultrasonics Sonochemistry 27 (2015) 408–415

Contents lists available at ScienceDirect

Ultrasonics Sonochemistry

journal homepage: www.elsevier.com/locate/ultson

Ultrasound-promoted one-pot three component synthesis of tetrazoles catalyzed by zinc sulfide nanoparticles as a recyclable heterogeneous catalyst

Hossein Naeimi *, Fatemeh Kiani

Department of Organic Chemistry, Faculty of Chemistry, University of Kashan, Kashan 87317, Islamic Republic of Iran

ARTICLE INFO

Article history:
Received 19 May 2015
Received in revised form 13 June 2015
Accepted 14 June 2015
Available online 15 June 2015

Keywords:
Ultrasonic irradiation
Tetrazoles
Zinc sulfide nanoparticles
Cyclization
Primary amines

ABSTRACT

Ultrasound irradiation was applied for the appropriate and rapid synthesis of 1-substituted tetrazoles through cyclization reaction of various primary amines, sodium azide and triethyl orthoformate. This reaction was effectively catalyzed by ZnS nanoparticles as an efficient, recoverable and reusable catalyst. Compared with conventional methods, this method has the considerable advantages such as shorter reaction times, easier work-up, purer products with high yields and mild conditions. The ZnS nanoparticles catalyst is an excellent instance to replace Brønsted acids for the preparation of 1-substituted tetrazole derivatives in very short reaction times with excellent yields. The catalyst can be recovered and reused several times without significant loss of its catalytic activity.

© 2015 Elsevier B.V. All rights reserved.

1. Introduction

Tetrazoles and their derivatives have gained considerable attention because they have a wide range of applications in information recording systems in material science [1], medicinal chemistry [2], photography [3] and agriculture [4]. Pharmaceutical applications of tetrazoles include antiallergic, antimicrobial, sedatives [5], anti-inflammatory [6], anti-HIV [7], hormonal [8], lipophilic spacers [9] and diuretics activity [10]. Furthermore, a range of proline derived tetrazoles have been reported as an enantioselective catalyst in asymmetric synthesis; additionally, they play a very important role as ligands in coordination chemistry [11]. Tetrazole derivatives can be prepared by different methods. Generally, the most convenient and versatile procedure for the preparation of tetrazoles is the cycloaddition between nitriles, cyanates, cyanamides and azides [4]. Several methods have been reported for the synthesis of 1-substituted tetrazoles involve acid-catalyzed cycloaddition between hydrazoic acid and isocyanides [12]. Acid-catalyzed cycloaddition between isocyanides and trimethyl azide [13], acetic acid or trifluoroacetic acid have catalyzed cyclization between primary amines or their salts, and an orthocarboxylic acid ester and sodium azide [14,15]. Acidic ionic liquid [16], ytterbium triflate [17], zeolites [18], indium triflate [19], silica sulfuric acid [4] have catalyzed cyclization of an amine, triethyl orthoformate and sodium azide to afford tetrazoles. Unfortunately, all of these methods have some drawbacks such as long reaction times, use of expensive and toxic reagents and high boiling solvents, harsh reaction conditions, low yield, tedious work-up, and even the need for excess amounts of highly toxic and explosive hydrazoic acid [2]. Therefore, in order to overcome these drawbacks, it is necessary to develop a simple, convenient and more efficient method for the synthesis of tetrazoles.

Recently, nanostructured materials have attracted much attention because of their unique properties that distinguish them from the bulk materials [20]. ZnS is one of the very important materials applied in organic synthesis with excellent catalytic activity [3]. In 2010, Lang et al. have been used mesoporous ZnS nanospheres as a new heterogeneous catalyst for the synthesis of 5-substituted 1H-tetrazole derivatives from various nitriles and sodium azide in DMF as a solvent [3].

In recent years, ultrasound has been extensively applied as a fantastic tool for different types of chemical reactions [21]. Acoustic cavitation is a physical phenomenon that promotes chemical reactions under ultrasound irradiation. This phenomenon includes the formation, growth, and implosive collapse of bubbles in a liquid during a very short period of the time. Precipitate implosion of these bubbles in the liquids generates localized hot spots with very short lifetimes. The hot spot has an equivalent temperature of 5000 °C and pressure of about 2000 atmospheres.

* Corresponding author.
E-mail address: naeimi@kashanu.ac.ir (H. Naeimi).

http://dx.doi.org/10.1016/j.ultsonch.2015.06.008
1350-4177/© 2015 Elsevier B.V. All rights reserved.

These transient, localized hot spots run high energy chemical transformations [22,23].

In continuation of ongoing to our work on the application of ultrasound in the organic reactions [24–26], we decided to carry out the ultrasonication reaction of primary amines, sodium azide and triethyl orthoformate catalyzed by ZnS NPs as a recyclable catalyst.

2. Experimental

2.1. Materials

All commercially available reagents were used without further purification and purchased from the Merck Chemical Company in high purity. The used solvents were purified by standard procedure as followed; DMF: drying over $CaSo_4$ and distillation under reduced pressure, EtOAc: washing with aqueous 5% Na_2CO_3, then with saturated aqueous NaCl and drying with $MgSO_4$, MeOH: by fractional distillation, EtOH: drying over CaO and distillation under reduced pressure, and acetonitrile: drying over P_2O_5 and distillation.

2.2. Apparatus

IR spectra were recorded as KBr pellets on a Nicolet FT-IR spectrophotometer. ^1H and ^{13}C NMR spectra were recorded in $CDCl_3$ on a Bruker DRX-400 spectrometer with tetramethylsilane as internal reference. A BANDELIN ultrasonic HD 3200 with probe model KE 76, with the diameter of 6 mm, was used to produce ultrasonic irradiation and homogenizing the reaction mixture. Piezoelectric crystal of this kind of probe normally works in the range of 700 kHz, but by using some proper clamps, the output frequency of piezoelectric crystal have controlled and reduced to 20 kHz. Therefore, the induced frequency of probe to the reaction mixture is equal to 20 kHz. By changing the power of Tip the cavitations rate is displaced so that the Tip frequency under various amounts of power is constant. A thermal method was used for the calibration of ultrasonic power. XRD patterns were recorded by an X'PertPro (Philips) instrument with 1.54 Ångström wavelengths of X-ray beam and Cu anode material. Scanning electron microscope (SEM) of nanoparticles was performed on a FESEM Hitachi S4160. Transmission electron microscopy (TEM) was performed with a Jeol JEM 2100UHR, operated at 200 kV. Melting points obtained with a Yanagimoto micro melting point apparatus are uncorrected. The purity determination of the substrates and reaction monitoring were accomplished by TLC on silicagel polygram SILG/UV 254 plates (from Merck Company).

2.3. Synthesis of ZnS nanoparticles

ZnS nanoparticles were synthesized according to the previously reported method [27]. Zinc nitrate hexahydrate (0.01 mol) was dissolved in 20 ml of propylene glycol under intensive stirring at 90 °C. Then, 10 ml of thioacetamide solution (1 M) was previously prepared and added dropwise to the solution over 10 min. Afterward, the solution was exposed to irradiate at microwave oven followed a working cycle of 50 s. (on) and 100 s. (off) at 350 W. After completion of the reaction, the mixture was slowly cooled to room temperature. The precipitate was filtered and consecutively washed with deionized water (5 × 50 ml) and absolute ethanol (3 × 10 ml) and was dried at room temperature.

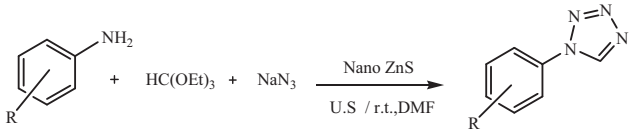

Scheme 1. Synthesis of 1-substituted 1*H*-1,2,3,4-tetrazoles by ultrasound irradiation and ZnS nanoparticles.

2.4. General procedure for synthesis of 1-substituted 1H-1,2,3,4-tetrazoles

A mixture of selected primary amine (1 mmol), triethyl orthoformate (1.2 mmol) and sodium azide (1 mmol) in the presence of 0.01 g ZnS nanoparticles was added to *N*,*N*-dimethylformamide as solvent and the reaction mixture was irradiated in ultrasonic apparatus with the power 50 W. The progress of the reaction was monitored by thin layer chromatography (TLC). After completion of the reaction, the mixture was diluted by 1:1 H_2O:ethylacetate (10 ml), stirred at ambient temperature (20 min) and centrifuged to separate the solid catalyst. The organic layer of the solution was separated, dried over sodium sulfate, and the organic solvent and other residues were stripped in a vacuum evaporator. The product was purified by recrystallization in a mixture of EtOAc:MeOH (3:1) to yield pure product. The obtained pure tetrazoles were characterized by spectroscopic data and melting points.

2.5. Spectral data for 1-substituted 1H-1,2,3,4-tetrazoles derivatives

2.5.1. 1-phenyl-1H-1,2,3,4-tetrazole

Yellow solid. m.p = 63–65 °C; IR (KBr)/ν (cm^{-1}): 3 051 (C–H, sp^2 stretch Ar), 1677 (C=N), 1588, 1488 (C=C); ^1H NMR (400 MHz, $CDCl_3$) δ ppm = 7.07–7.34 (m, 5H, *ArH*), 8.20 (s, 1H *tetrazole*).

2.5.2. 1-(4-Boromophenyl)-1H-1,2,3,4-tetrazole

White solid. m.p = 183–185 °C; IR (KBr)/ν (cm^{-1}): 3151 (C–H, sp^2 stretch, Ar), 1659 (C=N), 1576, 1481 (C=C); ^1H NMR (400 MHz, $CDCl_3$) δ ppm = 6.92–6.94 (d, 2H, *ArH*), 7.40–7.42 (d, 2H, *ArH*), 8.09 (s, 1H *tetrazole*); ^{13}C NMR (100 MHz, $CDCl_3$) δ ppm = 116.43, 120.76, 132.03, 143.99, 149.29.

2.5.3. 1-(4-Methylphenyl)-1H-1,2,3,4-tetrazole

Light yellow solid. m.p = 93–94 °C; IR (KBr)/ν (cm^{-1}): 3022 (C–H, sp^2 stretch, Ar), 2918 (C–H, sp^3 stretch), 1664 (C=N), 1607, 1506 (C=C); ^1H NMR (400 MHz, $CDCl_3$) δ ppm = 2.34 (s, 3H, *Me*), 6.94–6.96 (d, 2H, *ArH*), 7.11–7.13 (d, 2H, *ArH*), 8.17 (s, 1H *tetrazole*); ^{13}C NMR (100 MHz, $CDCl_3$) δ ppm = 20.79, 119.08, 129.63, 130.17, 142.95, 149.77.

2.5.4. 1-(3-Methylphenyl)-1H-1,2,3,4-tetrazole

White solid. m.p = 112–114 °C; IR (KBr)/ν (cm^{-1}): 3066 (C–H, sp^2 stretch, Ar), 2920 (C–H, sp^3 stretch), 1680 (C=N), 1598, 1483 (C=C); ^1H NMR (400 MHz, $CDCl_3$) δ ppm = 2.33 (s, 3H, *Me*), 6.86 (s, 1H, *ArH*), 6.89–6.91 (d, 2H, *ArH*), 7.18–7.22 (t, 1H, *ArH*), 8.21 (s, 1H *tetrazole*); ^{13}C NMR (100 MHz, $CDCl_3$) δ ppm = 21.43, 115.93, 119.97, 124.06, 129.19, 139.26, 145.28, 149.23.

2.5.5. 1-(2-Methylphenyl)-1H-1,2,3,4-tetrazole

White solid. m.p = 153–155 °C; IR (KBr)/ν (cm^{-1}): 3015 (C–H, sp^2 stretch, Ar), 2870 (C–H, sp^3 stretch), 1664 (C=N), 1488, 1590 (C=C); ^1H NMR (400 MHz, $CDCl_3$) δ ppm = 2.33 (s, 3H, *Me*), 7.02–7.03 (d, 1H, *ArH*), 7.05–7.07 (d, 1H, *ArH*), 7.18–7.22 (t, 2H, *ArH*), 8.08 (s, 1H *tetrazole*); ^{13}C NMR (100 MHz, $CDCl_3$) δ ppm = 17.94, 117.68, 123.43, 127, 128.71, 130.72, 144.10, 147.78.

2.5.6. 1-[4-(1H-tetrazol-1-yl)phenyl]ethanone

Yellow solid. m.p = 148–150 °C; IR (KBr)/ν (cm^{-1}): 3075 (C–H, sp^2 stretch, Ar), 2995 (C–H, sp^3 stretch), 1669 (C=N), 1499, 1585

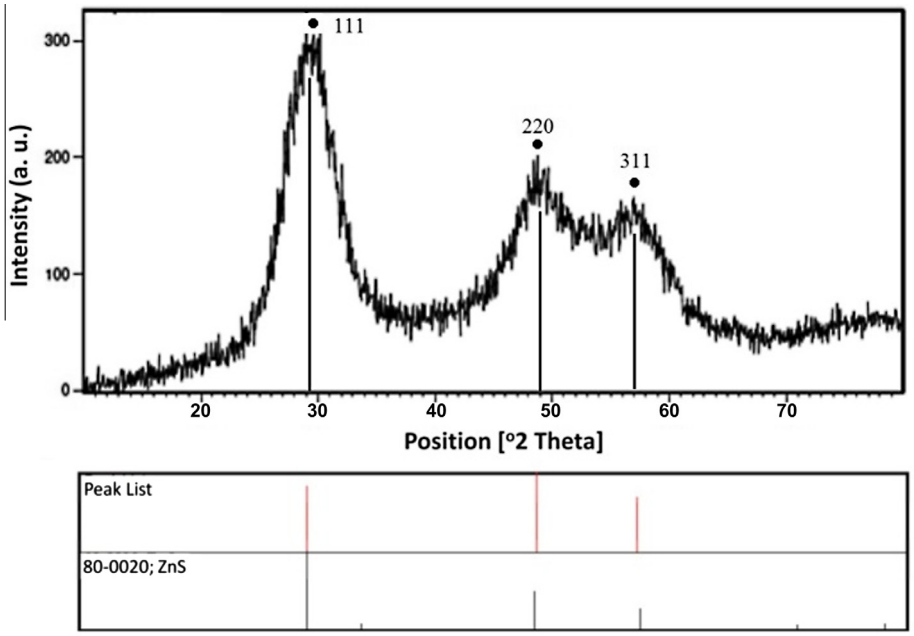

Fig. 1. The XRD pattern of zinc sulfide nanoparticles.

Table 1
Calculated structural parameters of ZnS nanoparticles from XRD data.

Parameters	Position (°2θ)	Plane (hkl)	FWHM (°2θ)	ε_{str}	D (nm)	δ (lines/m)	d_{hkl} (Å)
Values	28.8566	111	1.4170	45×10^{-3}	17.03	8.25×10^{16}	5.40
	48.7168	220	2.3616				
	57.0200	311	2.8800				

(C=C); ^{1}H NMR (400 MHz, $CDCl_3$) δ ppm = 2.60 (S, 3H, *Me*), 7.13–7.15 (d, 2H, *ArH*), 7.95–7.97 (d, 2H, *ArH*), 8.30 (s, 1H *tetrazole*).

2.5.7. 1-(2,4-Dimethylphenyl)-1H-1,2,3,4-tetrazole

White solid. m.p = 133–135 °C; IR (KBr)/ν (cm^{-1}): 3069 (C–H, sp^2 stretch, Ar), 2914 (C–H, sp^3 stretch), 1663 (C=N), 1495, 1607 (C=C); ^{1}H NMR (400 MHz, $CDCl_3$) δ ppm = 2.29 (s, 3H, *Me*), 2.30 (s, 3H, *Me*), 6.94–6.96 (d, 1H, *ArH*), 6.98–7.00 (d, 1H, *ArH*), 7.02 (s, 1H, *ArH*), 8.00 (s, 1H *tetrazole*).

2.5.8. 1-(Naphthalene-1-yl)-1H-1,2,3,4-tetrazole

White solid. m.p = 181–183 °C; IR (KBr)/ν (cm^{-1}): 3048 (C–H, sp^2 stretch, Ar), 1658 (C=N), 1574, 1432 (C=C); ^{1}H NMR (400 MHz, $CDCl_3$) δ ppm = 7.23–8.27 (m, 7H, *ArH*), 8.36 (s, 1H *tetrazole*).

2.5.9. 1-[2-(1H-tetrazol-1-yl)phenyl]-1H-1,2,3,4-tetrazole

White solid. m.p = 167–169 °C; IR (KBr)/ν (cm^{-1}): 3062 (C–H, sp^2 stretch, Ar), 1619 (C=N), 1458, 1588 (C=C); ^{1}H NMR (400 MHz, $CDCl_3$) δ ppm = 7.30–7.70 (m, 4H, *ArH*), 8.11 (s, 1H *tetrazole*); ^{13}C NMR (100 MHz, $CDCl_3$) δ ppm = 115.76, 122.37, 138.50, 142.40.

2.5.10. 1-(4-Chlorophenyl)-1H-1,2,3,4-tetrazole

White solid. m.p = 153–155 °C; IR (KBr)/ν (cm^{-1}): 3052 (C–H, sp^2 stretch, Ar), 1661 (C=N), 1485, 1581 (C=C); ^{1}H NMR (400 MHz, $CDCl_3$) δ ppm = 6.98–7.00 (d-2H, *ArH*), 7.27–7.29 (d, 2H, *ArH*), 8.09 (s, 1H *tetrazole*); ^{13}C NMR (100 MHz, $CDCl_3$) δ ppm = 120.35, 128.85, 129.47, 143.52, 149.50.

2.5.11. 1-(2-Chlorophenyl)-1H-1,2,3,4-tetrazole

White solid. m.p = 129–131 °C; IR (KBr)/ν (cm^{-1}): 3047 (C–H, sp^2 stretch, Ar), 1664 (C=N), 1470, 1582 (C=C); ^{1}H NMR (400 MHz, $CDCl_3$) δ ppm = 7.03–7.50 (m, 4H, *ArH*), 8.10 (s, 1H *tetrazole*).

2.5.12. 1-(3-Chlorophenyl)-1H-1,2,3,4-tetrazole

White solid. m.p = 137–139 °C; IR (KBr)/ν (cm^{-1}): 3065 (C–H, sp^2 stretch, Ar), 1670 (C=N), 1469, 1589 (C=C); ^{1}H NMR (400 MHz, $CDCl_3$) δ ppm = 6.92–6.94 (d, 1H, *ArH*), 7.07–7.09 (d, 2H, *ArH*), 7.26–7.27 (t, 1H, *ArH*), 8.14 (s-1H *tetrazole*); ^{13}C NMR (100 MHz, $CDCl_3$) δ ppm = 117.45, 119.23, 123.73, 130.34, 135.12, 146.14, 149.72.

3. Results and discussion

As a part of our growing interest in sonochemistry, with the purpose of improving the synthesis of 1-substituted tetrazole derivatives, we decided to perform a systematic investigation on the synthesis of these heterocycles under significantly milder conditions.

In continuation of our recent studies on application of ZnS nanoparticles, we hereby report a new protocol for the synthesis of 1-substituted 1H-1,2,3,4-tetrazoles in the presence of ZnS nanoparticles as a stable heterogeneous catalyst under ultrasound irradiation at room temperature (Scheme 1).

3.1. Characterization of the ZnS nanocrystals

The microstructures of the synthesized zinc sulfide nanoparticles were confirmed by X-ray diffractometer (XRD), Diffuse

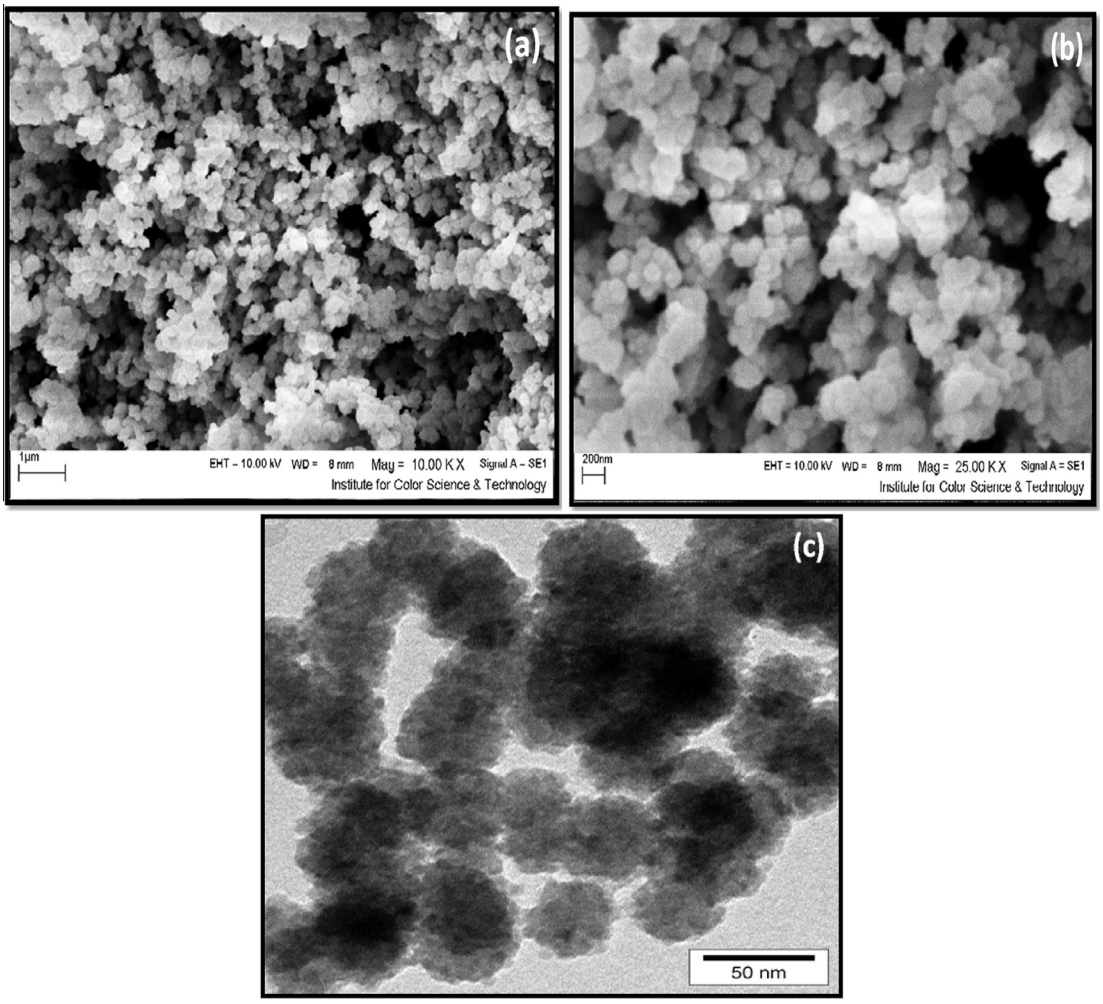

Fig. 2. SEM images of ZnS nanoparticles with two magnification (a and b) and TEM image of these nanoparticles materials (c).

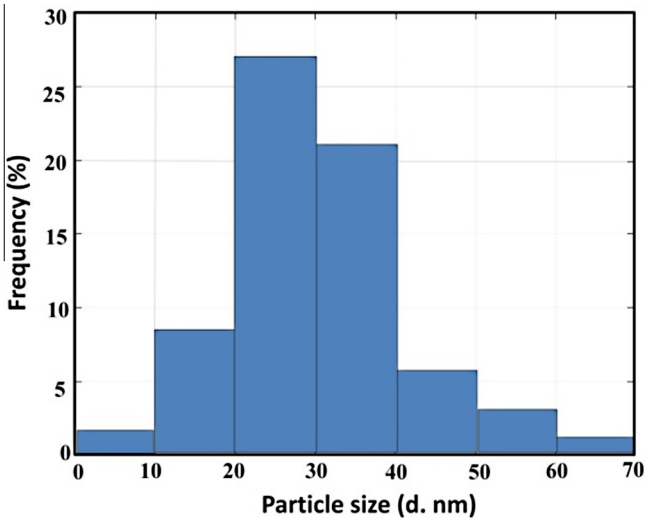

Fig. 3. Particle size distribution histogram of ZnS nanoparticles.

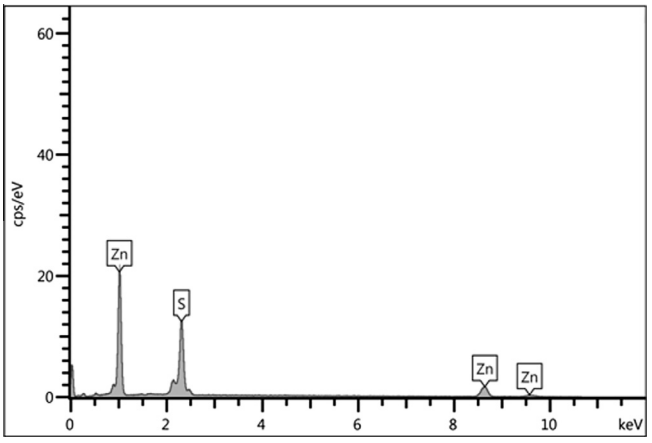

Fig. 4. Energy dispersive X-ray (EDX) spectra of ZnS nanoparticles.

Reflectance Spectroscopy (DRS), scanning electron microscope (SEM) and transmission electron microscope (TEM).

As revealed in Fig. 1, there are three broad peaks in the XRD pattern of the synthesized ZnS nanoparticles. The diffraction peaks at 2θ values of 28.8, 48.7, and 57.0 corresponds to (1 1 1), (2 2 0), and (3 1 1) diffraction planes of cubic ZnS, respectively. The average crystallite sizes of the zinc sulfide were estimated by Debye–Scherrer's equation; $D = 0.9\lambda/\beta\mathrm{Cos}\,\theta$, where D is the crystallite size, β is the full width at half maximum (FWHM) in radians of the diffraction peaks, θ is the Bragg's diffraction angle, and λ is the X-ray wave length (1.54056 Å). According to the FWHM of

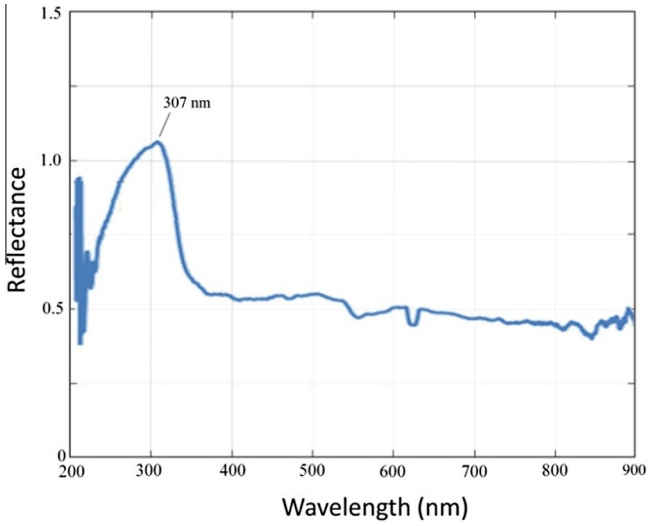

Fig. 5. UV–visible diffuse reflectance spectrum of ZnS nanoparticles.

the most intense (1 1 1) plane, the calculated crystallite size is found to be 17 nm. Additionally, the broadening of XRD peaks due to the FWHM is also related to the micro strain (lattice strain) that can be calculated by Stokes–Wilson equation; $\varepsilon_{str} = \beta \mathrm{Cos}\,\theta/4$ [28], where the values of β and θ are explained above. The pattern of the ZnS nanoparticles was indexed as a cubic phase which is very close to the values in the literature (JCPDS No. 80-0020 with cell constant $a = 5.3450$ Å). The amount of defects in the sample that naming as dislocation density (δ) was calculated by equation; $\delta = 1/D^2$, where D is the average crystallite size. Also, inter planer spacing was calculated using the relation $d_{hkl} = n\lambda/2\mathrm{Sin}\,\theta$. The calculated structural parameters are given in Table 1.

The very strong reflection peaks in the XRD pattern were shown that the ZnS nanoparticles were well crystallized. Also, there was detected any peaks in this pattern from other impurities such as ZnO or other compounds that confirmed the nanoparticles having pure phase.

As can be seen in Fig. 2, the images of both scanning electron and transmission electron microscopes were confirmed by the size of nanoparticles as 24–28 nm.

Fig. 3 shows the particle size distribution histogram from TEM image of the ZnS nanoparticles. As can be observed, the dispersed ZnS nanoparticles were formed with uniform size. From the size distribution histogram in Fig. 3, the mean value and standard deviation of nanoparticles size can be estimated as 27 ± 5 nm.

An Energy Dispersive X-ray Analyzer (EDX or EDA) was also used to check the elemental identification and quantitative compositional information of ZnS nanoparticles (Fig. 4). EDX was provided elemental analysis on areas as small as nanometers in diameter. The impact of the electron beam on the sample produces X-rays that are characteristic of the elements present on the sample. As shown in this figure, the presence of Zn L_α peak at 1.002 keV, Zn K_α peak at 1.560 keV, S L_α peak at 5.005 keV and S K_α peak at 1.560 keV could be observed. Also, no oxygen and other peaks (except Zn and S) for any other element have been found in the spectrum which confirmed that the ZnS nanoparticles are pure.

UV–visible diffuse reflectance spectrum of ZnS nanoparticles in the wavelength range of 200–900 nm was shown in Fig. 5. The band gap energy from UV-DRS was revealed the shift of band edge at shorter wavelength compared to the bulk ZnS (337 nm) due to the particle size of nano ZnS. The optical absorption edge of the ZnS nanoparticles at 307 nm (3.80 eV), is slightly blue shifted from that of the bulk ZnS (337 nm, $E_g = 3.65$ eV) [29]. This nearness of the absorption peak to the bulk ZnS crystals is attributed to the near band edge emission [30]. The broadening of the absorption spectrum could be due to the quantum confinement of the nanoparticles [31].

3.2. Optimization of the reaction conditions

In the present work, we investigated the effect of ultrasound irradiation on the model reaction of aniline, sodium azide and triethyl orthoformate in the presence of ZnS nanoparticles at room temperature (Table 2). Firstly, the effect of different solvents and various amounts of catalyst on the model reaction was conducted. Several organic solvents such as acetonitrile, ethanol, DMF and H_2O were examined. According to data given in (Table 2, entry 4), DMF was the most efficient solvent for this reaction. No reaction was observed in the absence of catalyst without ultrasonic irradiation (Table 3, entry 1). When the reaction was performed at room temperature in the presence of ZnS nanoparticles and in the absence of ultrasonic irradiation, the product was obtained in lower yield and longer reaction time (Table 3, entry 2), while in the presence of ultrasonic irradiation and 0.05 g of the catalyst, the yield increased to 92% and the reaction time is reduced to 20 min (Table 3, entry 6). It was demonstrated that combination method (ultrasound

Table 2
Optimization in the presence of different solvents[a].

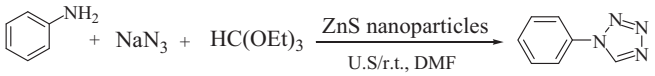

Entry	Solvent	Time (min)	Yield (%)[b]
1	Acetonitrile	30	62
2	EtOH	45	58
3	H_2O	45	63
4	DMF	20	92

[a] Reaction conditions: aniline 1.0 mmol, triethyl orthoformate 1.2 mmol and sodium azide 1.0 mmol.
[b] Isolated yields.

Table 3
Optimization of the various amount of catalyst[a].

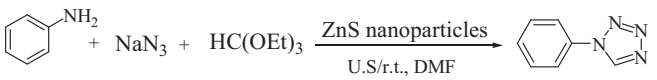

Entry	Condition	Nano ZnS (g)	Time (min)	Yield (%)[b]
1	Silent	–	120	0
2	Silent	0.01	120	12
3	US	0.01	85	45
4	US	0.03	50	61
5	US	0.04	35	78
6	US	0.05	20	92
7	US	0.07	20	92

[a] Reaction conditions: aniline 1.0 mmol, triethyl orthoformate 1.2 mmol and sodium azide 1.0 mmol.
[b] Isolated yields.

Table 4
Study of the effect of ultrasonic irradiation on the formation of tetrazole[a].

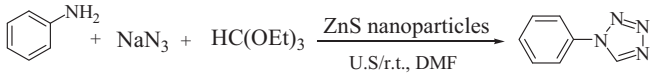

Entry	Power (W)	Time (min)	Yield[b] (%)
1	None[c]	120	12
2	30	85	54
3	40	65	68
4	45	40	83
5	50	20	92
6	55	20	92

[a] Reaction conditions: aniline 1.0 mmol, triethyl orthoformate 1.2 mmol and sodium azide 1.0 mmol.
[b] Isolated yields.
[c] The reaction without ultrasonic irradiation.

irradiation and ZnS nanoparticles) can be played an important role on the product yield and reaction time.

In continuation of this method, the role of ultrasonic irradiation and the effect of various powers of ultrasonic irradiation on the reaction were investigated. The reaction was performed in the presence of ZnS nanoparticles (0.05 g) as a catalyst in DMF, under silent condition and ultrasound irradiation (Table 4). The results illustrated that the sonication positively affected the reaction system. It could be reduce the reaction time and increase the yield of the products (Table 4, entry 2). While the reaction in the presence of ZnS nanoparticles without ultrasonic irradiation was carried out in low yield and long reaction time (Table 4, entry 1). Also, it was observed that the reaction in the presence of ZnS nanoparticles and ultrasonic irradiation with the power of 50 W gave the best result as the obtained product with 92% isolated yield during 20 min (Table 4, entry 5).

Ultrasonic irradiation differs from conventional energy sources. This incidence may be explained based on betterment of sorption on the catalyst surface and the better mass transport of organic compounds among the liquid phase and the catalyst surface under ultrasonic condition. These are ascribed to the shock wave and microjet manufactured by the cavitations. In term of sonication, dispersed ZnS nanoparticles in solution affords extra nucleation sites for acoustic cavity formation on its surface and gain the number of micro bubbles in the solution [32–35]. The quick implosion of these bubbles in the liquids generates localized hot spots with very short lifetimes. The high local temperature and pressures provide desirable conditions for driving a large number of chemical reactions. Thus, a wide variety of organic reactions can be performed in shorter reaction times with higher yields and milder conditions under ultrasound irradiation than with traditional methods.

After optimization of the reaction conditions, the limitation and generality of this work was investigated. For this aim, a variety of primary aromatic amines (1.0 mmol) containing electron donating and electron withdrawing substituents were reacted with triethyl orthoformate (1.2 mmol) and sodium azide (1.0 mmol) in the presence of ZnS nanoparticles optimum amount (0.05 g) under ultrasonic irradiation (50 W) and the desired 1-substituted-1H-tetrazole derivatives were obtained (Table 5). The results were shown that a wide range of aromatic amine derivatives containing electron withdrawing as well as electron donating groups produced corresponding tetrazoles in excellent isolated yields (Table 5).

Table 5
Synthesis of different tetrazoles from several amines[a].

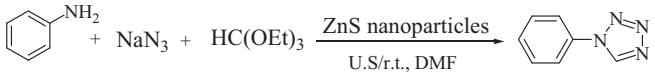

Entry	Primary amine	Product	Time (min)	Yield (%)[b]	Refs.
1	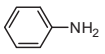	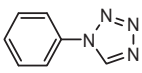	20	92	[17]
2	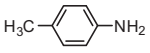	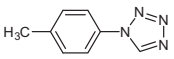	15	88	[17]
3	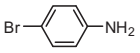	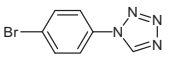	20	92	[36]
4	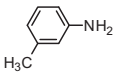	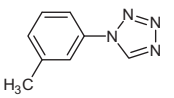	20	89	[17]
5	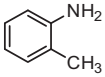	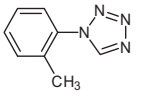	25	77	[17]
6	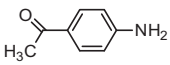	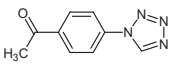	20	86	[16]
7	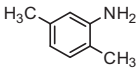	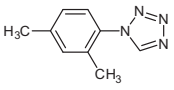	25	76	[36]
8		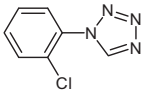	25	76	[17]
9	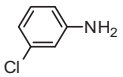	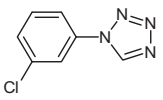	20	78	[37]
10	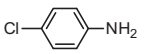	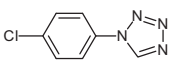	20	82	[17]
11		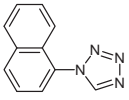	25	74	[17]
12	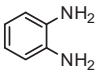	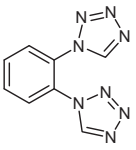	30	70	–

[a] Reaction conditions: aniline 1.0 mmol, triethyl orthoformate 1.2 mmol, sodium azide 1.0 mmol and ZnS nanoparticles 50 mol% (0.05 g).
[b] Isolated yields.

The comparison of results related to ultrasound irradiation with thermal conditions was indicated that, the reaction of various primary amines with triethyl orthoformate and sodium azide would be catalyzed by ultrasonic irradiation. As shown in Table 4, in the presence of ZnS nanoparticles, the excellent product yields were achieved in shorter reaction time under ultrasound irradiation. In

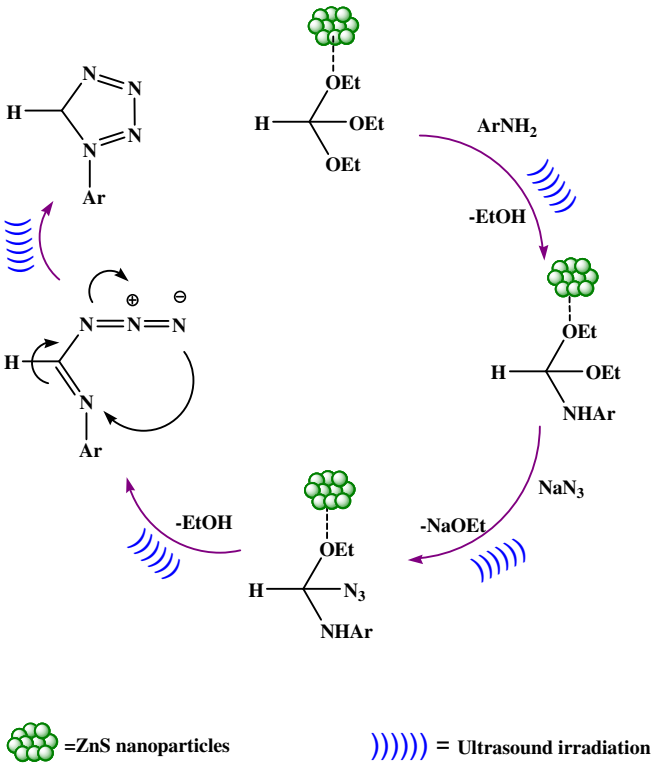

Scheme 2. The proposed reaction mechanism.

the previously reported work [27], the reaction of triethyl orthoformate and sodium azide with aniline or 4-chloro aniline catalyzed by ZnS nanoparticles in thermal conditions for 4.5 h and 4.7 h afforded 1-phenyl-1H-1,2,3,4-tetrazole and 1-(4-chlorophenyl)-1 H-1,2,3,4-tetrazole in 78% and 68% yields respectively (Table 3, entries 1 and 10) [27]. Whereas the present procedure needed only 20 min to result 1-phenyl-1H-1,2,3,4-tetrazole in 92% yield (Table 5, entry 1) and 20 min to result 1-(4-chlorophenyl)-1 H-1,2,3,4-tetrazole in 82% yield (Table 5, entry 10).

This method offered several advantages including simple reaction conditions, excellent yields, short reaction times, high purity, and the easy work up procedures. These results indicated that the ultrasound irradiation was an efficient method for the one-pot synthesis of 1-substituted tetrazoles as considerable and useful heterocycles.

3.3. The proposed reaction mechanism

The possible mechanism for the synthesis of 1-substituted 1H-tetrazol through catalyzed cyclization of aniline, sodium azide and triethyl orthoformate under ultrasonic irradiation in the presence of ZnS nanoparticles as catalyst is shown in Scheme 2. It is clear adsorption of triethyl orthoformate is improved on the ZnS nanoparticles surface by the effects of nano catalyst surface and also ultrasonic irradiation. Additionally, ultrasound can increases mass transfer of triethyl orthoformate between primary amine and sodium azide via the acoustic cavitation effect. The role of catalyst is activation of ethoxy groups and cleavage of C–O bonds. Generated carbonium ions can be stable through resonance by neighboring oxygen heteroatom or sequential nucleophilic displacements by amine and cyclization with azide.

In continuation of this research, the reusability and recyclability of the catalyst was investigated. The possibility of recovering and recycling of the catalyst is an important process from different aspects such as environmental concerns, and commercial

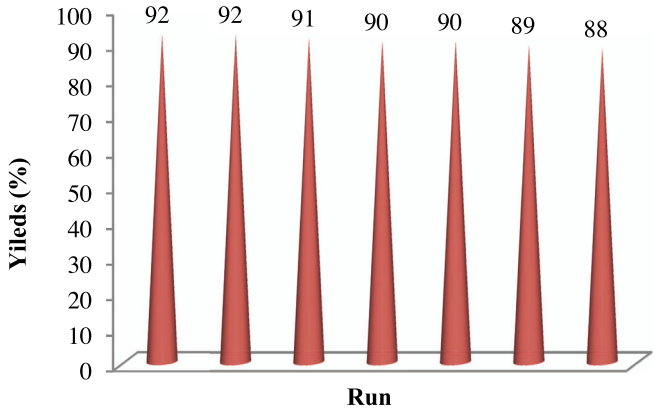

Fig. 6. Reusability of ZnS nanoparticles as catalyst toward synthesis of tetrazoles.

applicable processes. Therefore, we studied the recycling of the catalyst for synthesis of 1-substituted 1H-tetrazoles under optimized conditions. The aniline (1.0 mmol), triethyl orthoformate (1.2 mmol), sodium azide 1.0 mmol were sonicated in the presence of ZnS nanoparticles 50 mol% (0.05 g) in DMF as solvent (20 min). After completion of the reaction, the mixture was diluted by 1:1 H_2O/EtOAc (10 ml), stirred at ambient temperature (20 min) and centrifuged to separate catalyst. The solid catalyst was dried at 60 °C under reduced pressure to obtain almost quantitatively of the crude ZnS nanoparticles. After seven cycles, the catalyst was shown almost the same activity and gave the corresponding product in high yields Fig. 6.

4. Conclusion

In summary, we have described a mild, clean, fast, novel and safe sonochemical method for the synthesis of 1-substituted 1H-tetrazole derivatives by ZnS nanoparticles as a reusable and recoverable catalyst at room temperature. This novel protocol have significant advantages such as; high yields of desired products without side reactions, no elimination of hydrazoic acid as a toxic and explosive volatile gas, easy work-up and reusable catalyst. The catalyst can be separated by simple filtration and reuse several times without any significant loss of activity which is an additional sustainable characteristic of this method. The products have been confirmed by spectroscopic and physical data such as; IR, ^{1}H NMR, ^{13}C NMR and melting point.

Acknowledgment

The authors are grateful to University of Kashan for supporting this work by Grant No. 159148/56.

Appendix A. Supplementary data

Supplementary data associated with this article can be found, in the online version, at http://dx.doi.org/10.1016/j.ultsonch.2015.06.008.

References

[1] G. Qi, W. Liu, Z. Bei, Fe_3O_4/ZnS hollow nanospheres: a highly efficient magnetic heterogeneous catalyst for synthesis of 5-substituted 1*H*-tetrazoles from nitriles and sodium azide, Chin. J. Chem. 29 (2011) 131–134.

[2] M. Esmaeilpour, J. Javidi, F. Nowroozi Dodeji, M. Mokhtari Abarghoui, Facile synthesis of 1- and 5-substituted 1*H*-tetrazoles catalyzed by recyclable ligand complex of copper(II) supported on superparamagnetic Fe_3O_4@SiO_2 nanoparticles, J. Mol. Catal. A: Chem. 393 (2014) 18–29.

[3] L. Lang, B. Li, W. Liu, L. Jiang, Z. Xu, G. Yin, Mesoporous ZnS nanospheres: a high activity heterogeneous catalyst for synthesis of 5-substituted 1*H*-tetrazoles from nitriles and sodium azide, Chem. Commun. 46 (2010) 448–450.
[4] D. Habibi, H. Nabavi, M. Nasrollahzadeh, Silica sulfuric acid as an efficient heterogeneous catalyst for the solvent-free synthesis of 1-substituted 1*H*-1,2,3,4-tetrazoles, J. Chem. 2013 (2013) 4.
[5] S. Nag, S. Bhowmik, H.M. Gauniyal, S. Batra, Application of primary allylamines from Morita–Baylis–Hillman adducts: cyanogen azide mediated synthesis of substituted 5-aminotetrazoles and their attempted transformation into tetrazolo[1,5-a]pyrimidinones, Eur. J. Org. Chem. 2010 (2010) 4705–4712.
[6] S. Bepary, B.K. Das, S.C. Bachar, J.K. Kundu, A.S. Shamsur Rouf, B.K. Datta, Anti-inflammatory activity of indanyltetrazole derivatives, Pak. J. Pharm. Sci. 21 (2008) 295–298.
[7] E. Muraglia, O.D. Kinzel, R. Laufer, M.D. Miller, G. Moyer, V. Munshi, F. Orvieto, M.C. Palumbi, G. Pescatore, M. Rowley, P.D. Williams, V. Summa, Tetrazole thioacetanilides: potent non-nucleoside inhibitors of WT HIV reverse transcriptase and its K103N mutant, Bioorg. Med. Chem. Lett. 16 (2006) 2748–2752.
[8] J. Li, S.Y. Chen, S. Tao, H. Wang, J.J. Li, S. Swartz, C. Musial, A.A. Hernandez, N. Flynn, B.J. Murphy, B. Beehler, K.E. Dickinson, L. Giupponi, G. Grover, R. Seethala, P. Sleph, D. Slusarchyk, M. Yan, W.G. Humphreys, H. Zhang, W.R. Ewing, J.A. Robl, D. Gordon, J.A. Tino, Design and synthesis of tetrazole-based growth hormone secretagogue: the SAR studies of the O-benzyl serine side chain, Bioorg. Med. Chem. Lett. 18 (2008) 1825–1829.
[9] M. Nasrollahzadeh, Y. Bayat, D. Habibi, S. Moshaee, $FeCl_3$–SiO_2 as a reusable heterogeneous catalyst for the synthesis of 5-substituted 1*H*-tetrazoles via [2+3] cycloaddition of nitriles and sodium azide, Tetrahedron Lett. 50 (2009) 4435–4438.
[10] R.J. Nachman, G.M. Coast, K. Kaczmarek, H.J. Williams, J. Zabrocki, Stereochemistry of insect kinin tetrazole analogues and their diuretic activity in crickets, Acta Biochim. Pol. 51 (2004) 121–127.
[11] V. Rama, K. Kanagaraj, K. Pitchumani, Syntheses of 5-substituted 1*H*-tetrazoles catalyzed by reusable CoY zeolite, J. Org. Chem. 76 (2011) 9090–9095.
[12] D.M. Zimmerman, R.A. Olofson, The rapid synthesis of 1-substituted tetrazoles, Tetrahedron Lett. 10 (1969) 5081–5084.
[13] T. Jin, F. Kitahara, S. Kamijo, Y. Yamamoto, Copper-catalyzed synthesis of 5-substituted 1*H*-tetrazoles via the [3+2] cycloaddition of nitriles and trimethylsilyl azide, Tetrahedron Lett. 49 (2008) 2824–2827.
[14] Y. Satoh, N. Marcopulos, Application of 5-lithiotetrazoles in organic synthesis, Tetrahedron Lett. 36 (1995) 1759–1762.
[15] A.K. Gupta, C.H. Song, C.H. Oh, 1-(2-Iodophenyl)-1*H*-tetrazole as a ligand for Pd(II) catalyzed Heck reaction, Tetrahedron Lett. 45 (2004) 4113–4116.
[16] T.M. Potewar, S.A. Siddiqui, R.J. Lahoti, K.V. Srinivasan, Efficient and rapid synthesis of 1-substituted-1*H*-1,2,3,4-tetrazoles in the acidic ionic liquid 1-n-butylimidazolium tetrafluoroborate, Tetrahedron Lett. 48 (2007) 1721–1724.
[17] W.-K. Su, Z. Hong, W.-G. Shan, X.-X. Zhang, A facile synthesis of 1-substituted-1H-1,2,3,4-tetrazoles catalyzed by ytterbium triflate hydrate, Eur. J. Org. Chem. 2006 (2006) 2723–2726.
[18] D. Habibi, M. Nasrollahzadeh, T.A. Kamali, Green synthesis of the 1-substituted 1*H*-1,2,3,4-tetrazoles by application of the natrolite zeolite as a new and reusable heterogeneous catalyst, Green Chem. 13 (2011) 3499–3504.
[19] D. Kundu, A. Majee, A. Hajra, Indium triflate-catalyzed one-pot synthesis of 1-substituted-1*H*-1,2,3,4-tetrazoles under solvent-free conditions, Tetrahedron Lett. 50 (2009) 2668–2670.
[20] M. Muruganandham, R. Amutha, M. Sillanpää, Reagents for ZnS hierarchical and non-hierarchical porous self-assembly, ACS Appl. Mater. Interfaces 2 (2010) 1817–1823.
[21] D. Habibi, M. Nasrollahzadeh, L. Mehrabi, S. Mostafaee, P_2O_5–SiO_2 as an efficient heterogeneous catalyst for the solvent-free synthesis of 1-substituted 1*H*-1,2,3,4-tetrazoles under conventional and ultrasound irradiation conditions, Monatsh. Chem. 144 (2013) 725–728.
[22] T.J. Mason, Ultrasound in synthetic organic chemistry, Chem. Soc. Rev. 26 (1997) 443–451.
[23] M. Nasrollahzadeh, A. Ehsani, A. Rostami-Vartouni, Ultrasound-promoted green approach for the synthesis of sulfonamides using natural, stable and reusable natrolite nanozeolite catalyst at room temperature, Ultrason. Sonochem. 21 (2014) 275–282.
[24] H. Naeimi, K. Rabiei, Sonocatalyzed facile and mild one pot synthesis of gem-dichloroaziridine derivatives under alkaline conditions, Ultrason. Sonochem. 19 (2012) 130–135.
[25] R. Ghahremanzadeh, Z. Rashid, A.-H. Zarnani, H. Naeimi, A facile one-pot ultrasound assisted for an efficient synthesis of 1*H*-spiro[furo[3,4-b]pyridine-4,3′-indoline]-3-carbonitriles, Ultrason. Sonochem. 21 (2014) 1451–1460.
[26] H. Naeimi, Z.S. Nazifi, A facile one-pot ultrasound assisted synthesis of 1,8-dioxo-octahydroxanthene derivatives catalyzed by Brønsted acidic ionic liquid (BAIL) under green conditions, J. Ind. Eng. Chem. 20 (2014) 1043–1049.
[27] H. Naeimi, F. Kiani, M. Moradian, ZnS nanoparticles as an efficient and reusable heterogeneous catalyst for synthesis of 1-substituted-1*H*-tetrazoles under solvent-free conditions, J. Nanopart. Res. 16 (2014) 1–9.
[28] A. Khorsand Zak, W.H.A. Majid, M. Ebrahimizadeh Abrishami, R. Yousefi, R. Parvizi, Synthesis, magnetic properties and X-ray analysis of $Zn_{0.97}X_{0.03}O$ nanoparticles (X = Mn, Ni, and Co) using Scherrer and size–strain plot methods, Solid State Sci. 14 (2012) 488–494.
[29] S. Suresh, Synthesis, structural and dielectric properties of zinc sulfide nanoparticles, Int. J. Phys. Sci. 8 (2013) 1121–1127.
[30] M. Wang, L. Sun, X. Fu, C. Liao, C. Yan, Synthesis and optical properties of ZnS:Cu(II) nanoparticles, Solid State Commun. 115 (2000) 493–496.
[31] M. Ebrahimizadeh Abrishami, A. Kompany, S.M. Hosseini, N. Ghajari Bardar, Preparing undoped and Mn-doped ZnO nanoparticles: a comparison between sol–gel and gel-combustion methods, J. Sol–Gel. Sci. Technol. 62 (2012) 153–159.
[32] P. Gunasekaran, S. Perumal, P. Yogeeswari, D. Sriram, A facile four-component sequential protocol in the expedient synthesis of novel 2-aryl-5-methyl-2,3-dihydro-1*H*-3-pyrazolones in water and their antitubercular evaluation, Eur. J. Med. Chem. 46 (2011) 4530–4536.
[33] X. Wang, Y. Wei, J. Wang, W. Guo, C. Wang, The kinetics and mechanism of ultrasonic degradation of p-nitrophenol in aqueous solution with CCl_4 enhancement, Ultrason. Sonochem. 19 (2012) 32–37.
[34] D. Nagargoje, P. Mandhane, S. Shingote, P. Badadhe, C. Gill, Ultrasound assisted one pot synthesis of imidazole derivatives using diethyl bromophosphate as an oxidant, Ultrason. Sonochem. 19 (2012) 94–96.
[35] A. Javidan, A. Ziarati, J. Safaei-Ghomi, Simultaneous sonication assistance for the synthesis of tetrahydropyridines and its efficient catalyst ZrP_2O_7 nanoparticles, Ultrason. Sonochem. 21 (2014) 1150–1154.
[36] A. Khalafi-Nezhad, S. Mohammadi, Highly efficient synthesis of 1- and 5-substituted 1*H*-tetrazoles using chitosan derived magnetic ionic liquid as a recyclable biopolymer-supported catalyst, RSC Adv. 3 (2013) 4362–4371.
[37] S.N. Dighe, K.S. Jain, K.V. Srinivasan, A novel synthesis of 1-aryl tetrazoles promoted by employing the synergy of the combined use of DMSO and an ionic liquid as the solvent system at ambient temperature, Tetrahedron Lett. 50 (2009) 6139–6142.